Laser trapping mechanisms in nematic liquid crystal colloids

M. Škarabot[1], M. Ravnik[2], D. Babič[2], N. Osterman[2], I. Poberaj[2], S. Žumer [1,2], I. Muševič[1,2*]
[1] *J. Stefan Institute, Jamova 39, 1000 Ljubljana, Slovenia,*
[2] *Faculty of Mathematics and Physics, University of Ljubljana, Jadranska 19, 1000 Ljubljana, Slovenia*

A. Nych, U. Ognysta and V. Nazarenko
Institute of Physics, Prospect Nauki 46, Kyiv-22, 252022, Ukraine
(Dated: today)

We describe and analyze laser trapping of small colloidal particles in a nematic liquid crystal, where the index of refraction of colloids is smaller compared to the indices of the liquid crystal. Two mechanisms are identified that are responsible for this anomalous trapping: (i) surface-induced distortion of the birefringent media around the particle, creating a high-index "cloud" around the colloid, and (ii) laser induced distortion due to the local Freedericksz transition of a nematic, creating a "ghost" colloid. In majority of the experiments, the trapping above the Freedericksz transition is highly anisotropic. A very good agreement is found with a numerical analysis, considering nematic director elastic distortion, dielectric director-light field coupling and optical repulsion due to low index colloid in a high index surroundings.

PACS numbers:

I. INTRODUCTION

The long range nature of the orientational order in liquid crystals is responsible for many fascinating optic, electro-optic and mechanical properties of liquid crystals. Recently, there has been an increased interest in novel liquid crystalline systems such as the inverted nematic emulsions [**?** **?** **?**] and nematic liquid crystal colloids [**?** **?**]. It has been observed that the presence of small particles of a regular shape (i.e. colloids, water droplets) in an otherwise homogeneous nematic host gives rise to new, anisotropic structural forces, not observable in any other isotropic host. Being of an anisotropic nature, the interactions between inclusions induce growth of unique self-assembled structures such as linear chains [**?** **?**], 2D hexagonal arrangements of particles at interfaces [**?** **?**], or regular arrays of defects [**?**]. The unique combination of long-range anisotropic structural forces in liquid crystals and their electro-optic properties could therefore lead not only to new self-assembled structures for controllable photonic devices, but also to novel soft solids with unusual mechanical properties [**?**].

The nature of the interaction between objects in nematic liquid crystals has so far been studied both theoretically and experimentally. The theoretical studies have been concentrated mainly on two-body interactions, neglecting many-body corrections, and using either analytical [**?** **?** **?** **?** **?** **?** **?** **?** **?** **?**] or fully numerical approach [**?** **?** **?** **?** **?**]. The analytical, in most cases multipole-expansion approach, is expected to be valid in the far-field regime, i.e. at large interparticle separations, where the perturbation of the inclusions is small. In this picture, the object in a liquid crystal is considered as a static source of either monopole, dipole or quadrupole field that interacts in a pairwise manner with another object in its vicinity. This approach is therefore analogous to the multipole interaction picture in electrostatics and predicts $1/r^2$ structural force between two monopoles, $1/r^4$ structural force between two dipolar-like objects, and $1/r^6$ force between two topological quadrupoles. In comparison, fully numerical approach [**?**], found a good agreement for two parallel dipoles generating $1/r^4$ attractive force, whereas for two antiparallel dipoles, the numerically calculated repulsive force was stronger than expected from analytical considerations, $1/r^3$. The clear theoretical argument for the breakdown of the analytical approach is not available at this time, but is an indication of its limited validity.

The experiments were so far mainly concentrated on the study of dipolar and quadrupolar interactions in nematic colloids. Poulin et al. [**?**] have observed $1/r^4$ dipolar attractive forces between $2.8\mu m$ ferrofluid droplets in a nematic over a limited range of separation $9 - 18\mu m$. Yada et al. [**?**] have used laser tweezers to trap and measure forces between polystyrene colloids of micron size in low-index nematic. They have found $1/r^4$ attraction in a limited size of reduced separation $2 < R/a < 9$, which is very similar to recent experiments of Smalyukh et al. [**?**]. Laser tweezers were also used in the nematic colloidal experiments of Wood et al. [**?**] in a somewhat different context.

Recently Muševič et al.[**?**] have reported an unusual mechanism of laser trapping and manipulation of small colloids in the nematic liquid crystal. In that experiment, micron-sized glass particles with homeotropic boundary conditions were dispersed in the nematic liquid crystal with refractive indices that were larger compared to the index of refraction of colloids. Under such conditions, a repulsive force is expected to arise between a strongly focused light and the colloidal particle. As a surprise, the

*e-mail: igor.musevic@ijs.si

opposite was clearly observed: the colloid was attracted into the laser focus (trap) over extraordinary large separations of several microns. Two mechanisms were proposed to explain this forbidden trapping: (i) the trapping might be due to surface-induced distortion of the birefringent media around the particle, that creates a region of enhanced refractive index around the particle. For a particular polarization of the trapping beam, the particle is therefore "dressed with high index cloud" and behaves effectively as a high-index particle compared to surroundings. (ii) the second trapping mechanism includes local optical induced distortion of the order parameter of a birefringent fluid, or heating-induced reduction of the local order or even local melting of the nematic phase. This creates a "ghost" colloid at the laser focus, that interacts via structural forces with the real colloid.

In this paper we elaborate in detail the two proposed mechanisms and compare the experimental results with theoretical predictions using numerical approach. In the experimental part we first give a detailed description of the laser tweezers experiments followed by an extensive analysis of the observed trajectories of the colloids during many trapping experiments for different laser power. This is followed by an extensive analysis of the laser trapping potential, which turns out to be highly anisotropic in space. For certain range of colloidal separations and direction, we observe the Coulomb-like pair potential with an apparent $1/r$ separation dependence. In the theoretical section we present a numerical study of the interaction of the colloidal particle with a strongly focused laser light, where the laser-induced local Freedericksz transition is taken into account. We show that this scenario reproduces an effective $1/r$ dependence of the trapping potential in a certain direction very well. The analysis shows that the Coulomb-like potential is reproduced only for a very specific direction of the pair potential and is a result of the combination of several interaction terms.

II. EXPERIMENT

The experiments have been performed using silica spheres of diameter $2a = 0.97\mu m$, and the refractive index $n_s = 1.37$, that were dispersed in a nematic liquid crystal $4' - n -$ pentyl $4 -$ cyanobiphenyl (5CB) with refractive indices $n_0 = 1.53$ and $n_e = 1.70$ at room temperature. Some of the experiments have also been performed in E12, which is an eutectic mixture of n-cyanobiphenyls with a clearing temperature of 59^oC. At room temperature, the ordinary index of refraction of E12 is $n_o = 1.52$, the extraordinary index is $n_e = 1.74$, both are therefore higher than the refractive index of silica spheres.

The surface of the spheres was first covered with a monolayer of N,N-dimethyl-N-octadecyl-3-aminopropyltrimethoxysilyl chloride (DMOAP) that ensures very strong homeotropic surface anchoring of a nematic liquid crystal. The particles were then introduced into the nematic liquid crystal and analyzed under the polarizing microscope. An image of somewhat larger ($4\mu m$) colloidal particle in a 5CB homeotropic cell under crossed polarizers is shown in Fig. 1a, whereas the same type of particle in a 5CB planar cell is shown in Fig. 1b. We should comment that very similar structures were observed for $0.97\mu m$ silanated silica colloids, only the image quality was worse.

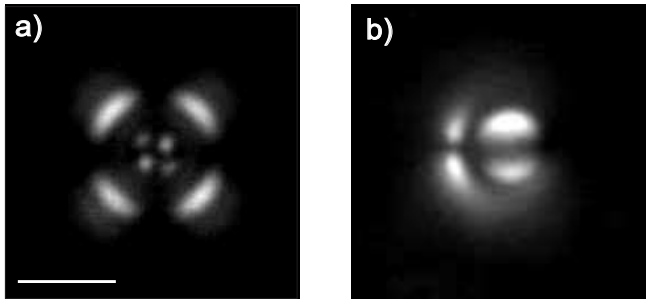

FIG. 1: (a) Polarization micrograph of a $4\mu m$ diameter silica colloid treated with DMOAP in a homeotropic cell of 5CB. The dipolar field distribution around the colloid cannot be resolved, because the dipolar axis is along the director, i.e. perpendicular to the plane of the paper. The hedgehog is therefore either positioned above or below the colloid. The scale corresponds to $5\mu m$. (b) The same type of colloid in a planar 5CB cell clearly shows the dipolar director distribution. The same type of ordering is observed for $0.97\mu m$ colloids.

The two images clearly show the dipolar character of the director field around the silane-treated colloids in the nematic. The nematic colloidal dispersion was heated into the isotropic phase, intensively sonicated to obtain homogeneous dispersion of isolated colloidal particles and then introduced into a glass cell using capillary force. When preparing the colloidal dispersion, the volume concentration of the colloidal particles should be very low, of the order of $1ppm$. Such a low concentration prevents buckling of the colloids during the cooling and phase transitions. We have used cells made of soda-lime glass plates of thickness $0.15mm$ that were also covered with DMOAP to assure good homeotropic alignment of the LC. Cells of different thicknesses were used in the experiments, ranging from 10 to $50\mu m$.

We have used a laser tweezers setup built around an inverted microscope (Zeiss, Axiovert 200 M) and a CW diode-pumped solid-state laser (Coherent, Compass 2500 MN) at 1064 nm was used as a laser source. An acousto optic deflector (AOD, IntraAction, model DTD-274HA6)), driven by computerized system (Aresis, Tweez Tek 70) was used for trap manipulation. A beam expander was used to match the laser beam to the AOD aperture and some additional optics was used to image the pivotal point of the AOD onto the entrance pupil of the water immersion microscope objective (Zeiss, IR Achroplan 63/0.9W). The maximum laser power of a diffraction limited beam in the sample plane was up to $64mW$. The laser light was linearly polarized and two or-

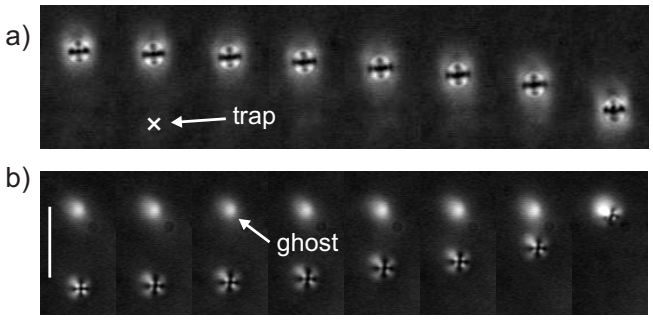

FIG. 2: Sequences of micrograph images under crossed polarizers, showing two different trapping events in 5CB. The scale bar is $10\mu m$ and is equal for both images. Note the apparent size of a $0.97\mu m$ diameter colloid under crossed polarizers. (a) trapping at low power of $25mW$, which is below the power that is necessary to induce the local optical Freedericksz transition. The cross indicates the position of the optical trap, which is not visible. (b) trapping at $35mW$, which is above the optical Freedericksz transition. The bright spot is due to local birefringent area, created by the laser light induced distortion of the director field.

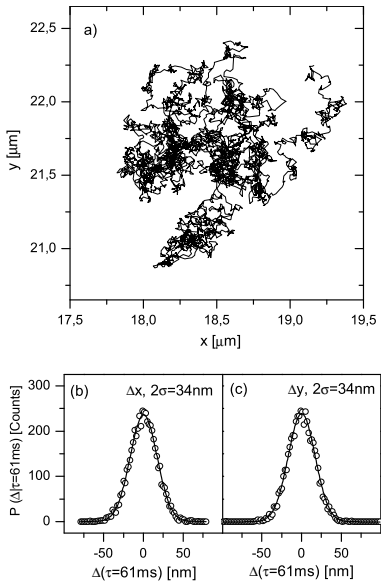

FIG. 3: (a) Recorded trajectory during the Brownian motion of a silanated $0.97\mu m$ silica colloid in a homeotropic cell filled with 5CB. (b) and (c) represent histograms of particle's displacements between two consecutive positions, separated by a time interval of $61ms$, along the two perpendicular directions. The solid lines are Gaussian fits with $2\sigma = 34(1 \pm 0.01)nm$. There is no difference between the x and y directions.

thogonal polarizations could be selected using a rotating half-wave plate.

Once an isolated particle was selected, the tweezers focus was positioned close to the particle. The separation was set approximately to $10\mu m$, and the movement of the particle towards the laser focus was video monitored at a rate of 20 frames/s. At low power levels (up to $25mW$ for 5CB), i.e. below the power level for Freedericksz transition, the particle attraction was observed over separations of around $5\mu m$. As we have found that the particle was always attracted along the direction of polarization of the laser light, we have concluded, that the particle is trapped via its "birefringent cloud", shown in Fig.1. Namely, due to distorted director field in the close vicinity of the colloid, there is a region of enhanced refractive index for a given polarization of the laser beam with respect to homeotropic surroundings. The region of enhanced refractive index is positioned symmetrically with respect to the center of the colloid and there are two energy minima very close to the surface of the colloid where the colloid is trapped.

At slightly higher laser power we have observed a much stronger trapping that was efficient over separations of more than ten micrometers. Under unpolarized imaging, it appeared as if the colloid was attracted by another, invisible, i.e. "ghost" colloid, positioned at the focus point. However, the nature of this "ghost" colloid was revealed by observing the trapping event under crossed polarizers, as shown in the series of polarized micrograph images in Figures 2a and 2b. Figure 2a shows a trapping event below the threshold for Freedericksz transition, where the position of the laser trapped cannot be resolved, as there is no optical-induced deformation of the director field. However, one can clearly see, that when the laser power was increased above the Freedericksz threshold, significant distortions of the director field around the laser focus were observed (bright spot in Figure 2b). This distorted region therefore acts as a long-range trapping site, attracting the particle over several micrometers.

In an off-line analysis, the position of the center of gravity of the particle was determined by a computer video-analysis of the captured frames with an accuracy of $\pm 3nm$. Having the recorded time-dependence of the separation between the particle and the laser focus, it was possible to restore the effective elastic pair potential between the particle and the laser trap. Following the Stokes law, the drag force $F = 6\pi R_{eff}\eta\partial r/\partial t$ is nearly balanced with the attractive force from the laser focus. The resulting unbalanced acceleration corresponds only to a fraction of both forces. The force between the focus of the laser tweezers and the silica particle was therefore calculated from the recorded time series of the particle's positions. Finally, by integrating the calculated drag force over the separation, we could determine the interaction pair potential. This analysis was performed on several tens of trapping experiments, leading basically to identical results.

In addition to trapping experiments, we have also performed a Brownian motion experiment, similar to Loudet et al. [**?**], where the product of the effective radius and viscosity $6\pi R_{eff}\eta$ could be determined. This was done simply by recording and analyzing Brownian motion of the colloid in the absence of the laser light. As an example, we show in Figure 3a the trajectory of the colloid in a homeotropic cell filled with 5CB during the time in-

terval of 300 sec, showing in total around 5000 recorded positions. The time interval τ between the two neighboring positions is $\tau = 61ms$. Figures 3b and 3c show the corresponding histograms of particle displacements in two perpendicular directions. It is clearly a Gaussian distribution with a width of $2\sigma = 34(1 \pm 0.01)nm$. The self-diffusion coefficient D of thermal motion is related to the width of the distribution σ and the time τ between two consecutive steps via $D = \frac{\sigma^2}{\tau}$ [**?**]. Finally by using Stokes-Einstein relation we can determine the product of the effective radius and viscosity, which is in our case $R_{eff}\eta = 4.6\times10^{-8}kgs^{-1}$ for $2a = 0.97\mu m$ silanated silica spheres in 5CB at room temperature.

In all experiments performed and in the range of laser power above the optical Freedericksz transition, we have observed basically two different types of trajectories of particles during the trapping event. These are shown ing Figs. 4a-c. Figures 4a and 4b show the 'spider' like trajectories that were observed in approximately 80 percents of the experiments. The 'star' like trajectories shown in Fig. 4c were observed in approximately 20 percents of our experiments, where, in total more than 20 trapping experiments have been performed. The different symmetries of the two types of trajectory indicate two different symmetries of the director field around the colloid. We conclude that we have around 80 percents of cases where the director field has no mirror symmetry with respect to x-y plane (see Figure 5) and 20 percents of cases where this mirror symmetry is realized. The first case indicates that strong colloidal surface anchoring induces dipole-like director distortion. The latter case most probably corresponds to the weaker surface anchoring, where quadrupole-like director distortion is realized.

In this paper we study in detail more abundant cases with spider-like trajectories shown in Figs. 4a and 4b that are observed above the optically-induced local Freedericksz transition. The silica particle was released from the positions labelled 1-8 in a random sequence and the laser spot was in the center. Clearly, the silica particles follow the shortest trajectory towards the laser focus only for certain directions, which we call an "easy direction". In other cases, there is a direction where the silica and "ghost" particles demonstrate repulsive interaction. In this case of a "hard direction", the particle avoids repulsion and takes a 'detour' trajectory that ends in the laser focus. More precisely, measurement on larger ($4\mu m$) colloids indicates that the position of the center of the trap is very close to the surface of the colloid, where the repulsion due to smaller index of refraction of the silica colloids becomes important. After changing the direction of polarization of the trapping beam, the set of trajectories is rotated by 90 degrees as a whole. Since the polarization defines the two equivalent directions whereas we observe only one particular direction, one may conclude that the interaction depends on the exact deformation of the director produced by the laser irradiation.

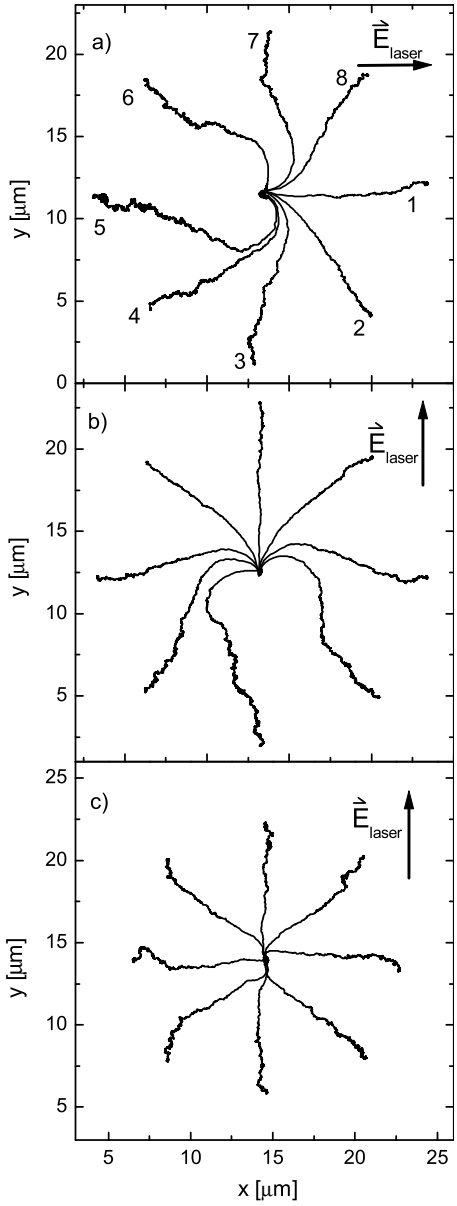

FIG. 4: (a) "Spider-like" trajectories during the optical trapping of a $0.97\mu m$ silica colloid in a homeotropic 5CB cell. The laser power is $35mW$ (i.e. above the optical Freedericksz transition) and the starting positions are labelled 1-8. (b) The set of "spider-like" trajectories rotates as a whole, as the polarization of the laser light is rotated by 90°. (c) Trapping of the same type of colloid at the same laser power, that is observed in approximately 20 percents of the experiments. The spider-like trajectories correspond to dipole director field around the colloid, whereas the 'star-like' trajectories shown in (c) indicate quadrupole symmetry of the director field around the colloid.

III. THEORY

In this Section we consider all the relevant distortions of the director field and couplings to the external field in the experimental geometry shown in Figure 5. We

consider that the laser beam induces local Freedericksz transition of the director field in the laser focus and combine this field with the one of the colloid. This is a complete modelling of the effective electro-elastic potential that acts on a colloidal particle close to the laser trap. The calculation is based on a numerical integration of the free energy density consisting of three contributions: (i) elastic interaction due to deformed nematic director field around the colloid and the trap (Frank's elasticity), (ii) the dielectric interaction of an inhomogeneous and anisotropic director field with an inhomogeneous electric field of the focused light, and (iii) the repulsive dielectric interaction of a colloid (with a small refractive index) with an inhomogeneous electric light field. Till now each of these interactions has been studied separately [**?**] [**?**].

In the one elastic constant approximation, the free energy is:

$$\begin{aligned} F = & -\frac{1}{2}K\int_{D^{LC}}\left(\frac{\partial n_i}{\partial x_j}\right)\left(\frac{\partial n_i}{\partial x_j}\right)dV \\ & -\frac{1}{2}\epsilon_a\epsilon_0\int_{D^{LC}}\left(\mathbf{n}(\mathbf{r})\cdot\mathbf{E}(\mathbf{r})\right)^2 dV \\ & +\frac{1}{2}(\epsilon_{LC}-\epsilon_C)\epsilon_0\int_{D^C}\mathbf{E}(\mathbf{r})^2 dV \quad , \end{aligned} \tag{1}$$

K is the average elastic liquid crystal constant, $\mathbf{r} = (x, y, z)$ is the position vector and x, y and z are the corresponding cartesian coordinates, $\mathbf{n}(\mathbf{r})$ is the director field, $\mathbf{E}(\mathbf{r})$ is the electric filed of the laser trap, ϵ_C is the dielectric constant of the colloid, $\epsilon_a = \epsilon_\parallel - \epsilon_\perp$ is the liquid crystal dielectric anisotropy for optical frequencies and $\epsilon_{LC} = (\epsilon_\parallel + \epsilon_\perp)/2$ is the corresponding average dielectric constant of the liquid crystal for optical frequencies. In the Eq. **??** the first two terms are integrated over the whole volume of the liquid crystalline medium (D^{LC}), while the third term is integrated over the volume of the colloid (D^C). Summation over repeated indices i, j is assumed.

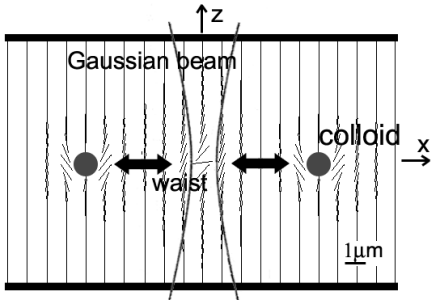

FIG. 5: Schematic picture of the interaction of a Gaussian light beam with a colloid in a homeotropic nematic cell. The beam induces an optical Freedericksz transition, which creates a region of a distorted director field inside the cell. This can be considered as a 'ghost' colloid that interacts with a real colloid. Note the difference in interaction for two opposite positions of the colloid. The director field of the colloid on the left side nearly "matches" the trap, whereas there is strong distortion and consequently repulsion for the colloid approaching from the right side. Note that there is no such difference for the interaction for colloids with quadrupolar director field.

Here we have considered that the electric field of the laser trap that interacts with the liquid crystal is time-independent. This is well justified since the modulation frequency of the laser trap electric field is in the range of $\sim 10^{14}$Hz, while 5CB director switching rate is at most in 10^3Hz range. We have also considered a single elastic constant approximation, which is justified, as in 5CB the elastic constants differ for at most $\sim 40\%$ [**?**]. In the calculation of the dielectric coupling of the colloid the average liquid crystal dielectric constant for optical frequencies ϵ_{LC} is used. Ordinary and extraordinary dielectric constants in 5CB differ for $\sim 10\%$ from the average value. For a more precise analysis the Mie scattering or other similar approaches should be used [**?**].

We have first determined the electric and the director fields for the optical trap and the colloid for different positions of the colloid and the trap. The Gaussian beam profile has been used, that is a typical description for strongly focused laser beams [**?**]. The electric field $\mathbf{E}(\mathbf{r})$ of the focused light beam is:

$$\mathbf{E} = \frac{\mathbf{E_0}}{\sqrt{\left(1+(\frac{z}{z_0})^2\right)}}\exp\left(-\frac{x^2+y^2}{w_0^2(1+(\frac{z}{z_0})^2)}\right) \quad , \tag{2}$$

Here $\mathbf{E_0}$ is the electric field amplitude of the linearly polarized light, w_0 is the radius of the waist and $z_0 = \pi w_0^2\sqrt{\epsilon_{LC}}/\lambda$ is the measure of near - (electric) field area, where λ is the wavelength of the laser light.

The director field has been determined in two steps. First the director field around the optical trap was numerically calculated from the Lagrange-Euler free energy minimization equations for the director field within a Gaussian beam (Eq. **??**). Here we have considered a local Freedericksz transition induced by strong light, as well as the homeotropic boundary conditions at the confining plan-parallel walls of the sample cell with very strong surface anchoring. In the second step, the director field of the optical trap (ghost colloid) was combined with the dipolar ansatz (dipolar approximation) for the director field $\mathbf{n}$ around a spherical colloid with radius a and homeotropic anchoring $\mathbf{n_{col}} \sim 3.08a^2(\mathbf{r}-\mathbf{R})/(r-R)^3$, which was first introduced by Stark *et al* in [**?**]. Here $\mathbf{R} = (X, Y, Z)$ stands for the position vector of the colloid. Finally, the combined normalized director field was used in the calculation of the free energy F. Schematic presentation of the Gaussian beam and the director field with the ghost and real colloid is given in Figure 5.

One could argue that the use of a linear polarization in the Gaussian beam is a very rude approximation since liquid crystals are well known birefringent materials that split light beams in ordinary and extraordinary rays. Nevertheless this is relevant only when the real and ghost

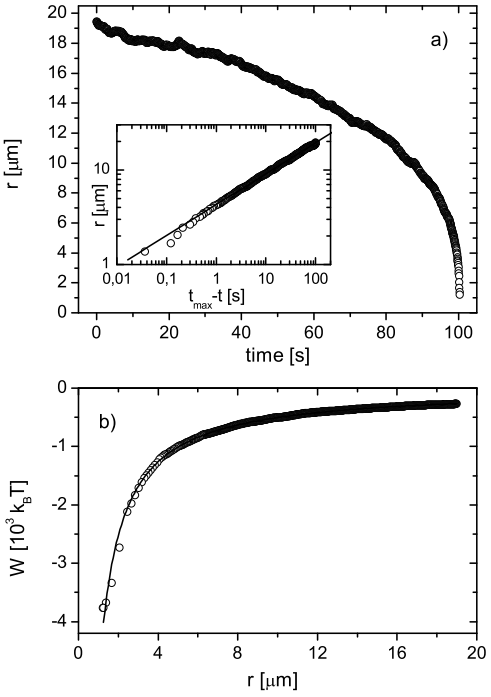

FIG. 6: (a) Recorded time dependence of the separation between a silica particle and the laser trap during the trapping event in a homeotropic 5CB cell at a laser power of $50mW$, starting from the "easy position" labeled 1 in Fig. 4a . The colloid is trapped at a time labelled t_{max}. The inset shows the log-log plot of the same data showing clear power-law dependence with an exponent $\alpha = 0.33(1 \pm 0.02)$. (b) The laser trapping potential derived from the data in (a). The solid line is the best fit to $W(r) = W_0/r$ with $W_0 = 5980(1 \pm 0.002)k_BT\mu m$.

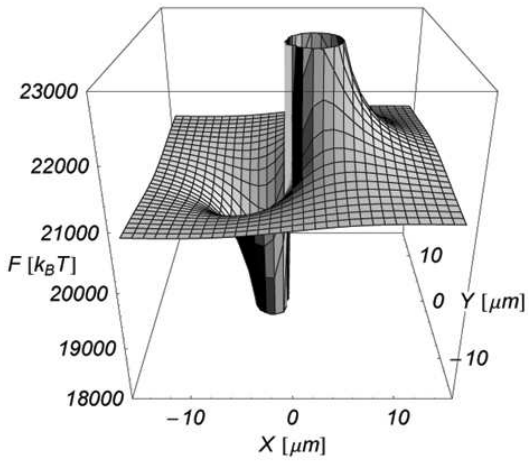

FIG. 7: The effective pair potential for the colloid in the vicinity of the laser trap at large laser power, i.e. above the local Freedericksz transition. The trap is centered at $X = Y = 0$, the light polarization is along the x-direction. The cell thickness is 20μm, $K = 6 \cdot 10^{-12}$N, $\epsilon_{\parallel} = 2.9$, $\epsilon_{\perp} = 2.3$, $\mathbf{E_0} = 8 \cdot 10^6$V/m $\mathbf{e_x}$, $w_0 = 0.5\mu$m, $\lambda = 1064$nm, $a = 0.5\mu$m, and $\epsilon_C = 1.7$.

colloid are very close (2-3 colloid radii) and the director can thus point in an arbitrary direction. When the real colloid is further away the director and consequently optical axis stay in the polarization plane. Light beam of the laser trap so "feels" only extraordinary refractive index and therefore only slightly deflects from its incident direction.

Therefore in our particular experiment this "beam - walkoff" effect is very small and the light beam deviates for less than 0.5μm when passing through the whole cell ($\sim 20\mu$m thick). The polarization thus stays linear and mainly unperturbed.

IV. RESULTS AND DISCUSSION

Figure 6a. shows the time dependence of the separation between the colloid and the laser trap at $P = 50mW$, when the colloid was released along the 'easy' direction, starting from the position 1 in Fig. 4a. The inset to Fig. 6a shows the log-log plot of the same data, clearly indicating the power-law dependence with an exponent $\alpha = 0.33(1 \pm 0.02)$. It can be shown that the exponent α describing the time-dependence of the separation $r(t) = A \cdot (t_{max} - t)^{\alpha}$ is related to the exponent β describing the separation dependence of the pair potential $W_p = W_0 \cdot r^{\beta}$ through $\beta = 2 - \frac{1}{\alpha}$ [**?**]. For $\alpha = 0.33(1 \pm 0.02)$ this gives Coulomb -like attraction with an exponent $\beta = -1.01(1 \pm 0.05)$. An extensive analysis of a set of several experiments on different samples and colloids basically confirms this Coulomb like attraction with an average exponent of $\beta = -0.99(1 \pm 0.06)$.

The separation-dependence of the interaction between the colloid and the laser trap was also analyzed by calculating the separation-dependence of the attractive force. After integrating the force over separation, the pair potential was calculated, as shown in Figure 6b. The potential is of the Coulomb-like type, as evidenced by a very good fit indicated by a solid line. The potential is extremely strong, reaching several thousands of k_BT at small separations.

Let us now compare the experimental data to the numerical calculations of the resulting effective potential of our optical trap, which are presented in Figures 7 and 8. The laser Gaussian beam propagates along the z axis at $X = Y = 0$. The values of the pair potential are calculated in the $Z = 0$ plane positioned at the separation 10μm from the cell wall (see Fig. **??**).

Figure 7. represents numerically calculated trapping potential above the local optically-induced Freedericksz transition. One can see that numerical calculations reasonably well explain the observed trajectories of the colloid trapping, shown in Figures 4. In most of the XY plane the colloid experiences an attractive potential of

the optical trap, that attracts it in a nearly straight line towards the trap. The starting point labelled 1 in Figure 4a therefore corresponds to the laser trapping from the left side of the potential well in Figure 7. However, as the numerically calculated potential is of an asymmetrical shape, the colloid is deflected from the straight direction, if it approaches the trap from the 'hard' direction. This is a direction from the far right side of the potential well in Figure 7, that corresponds to the position 5 in Figure 4a.

We have fitted the effective free energy F with a power law $a_0 + b_0/r_i^\alpha$, where i stands for X or Y and a_0, b_0 are constants. Along the 'easy' direction (-15μm $<$ X $<$ -1μm, Y $= 0$) we find $\alpha = 1.1$, which is close to the observed Coulomb-like exponent. Over the range of separation ($X = -1\mu$m$, 0 <$ |Y| $< 15\mu$m) we find $\alpha = 1.6$. Note that in the direction perpendicular to the polarization the attractive potential decays with a higher exponent, which is due to the anisotropy of the director field to electric field.

Numerical results of the potential strength are also in a rather good agreement with the experiment. Along the easy direction the potential drops to a minimum value of $\sim 3000 k_B T$ compared to zero potential far away. As a result, this potential drop gives rise to a typical $1pN$ force. We should stress that the strength of the potential depends strongly on the laser power, whereas its shape changes substantially only when the laser power is above the threshold for the local optical Freedericksz transition (see Fig. 7.).

Figure 8. shows the trapping potential at low power level, i.e. below the optical Freedericksz transition. The remaining asymmetry in the effective pair potential at low laser power is caused by the anisotropic dielectric director to electric field interaction. Along the direction of the polarization this interaction is stronger as in the perpendicular direction, which results in two potential minima positioned symmetrically along the direction of polarization. The reason is in the director field in the close vicinity of the colloid, which is parallel to the light polarization only in two localized regions close to the colloidal surface.

Finally, we should emphasize that the observed Coulomb-like exponent for the attraction along the easy direction is a result of a combination of several interactions: (i) the elastic anisotropic attraction between the laser-distorted nematic in the laser waist and the elastically deformed region around the colloid, (ii) the anisotropic dielectric attraction of the laser polarization with distorted and optically anisotropic nematic, and (iii) the symmetric and repulsive interaction between the low index colloid and the laser waist. The combination of these three interactions gives rise to an effective Coulomb-like attraction, which is however observable only for certain direction and range of separations where the screening caused by the confinement of the nematic in a homeotropic cell is still negligible. In other directions, the effective exponent of the pair potential is quite different and even changes sign.

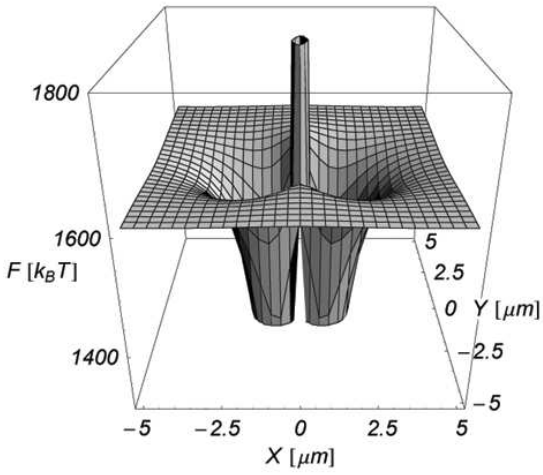

FIG. 8: The effective potential for the colloid approaching the laser trap below the local Freedericksz transition. The trap is centered at $X = Y = 0$, the light polarization is along the x-direction. The following parameters were used in numerical calculation: $K = 6 \cdot 10^{-12}$N, $\epsilon_\parallel = 2.9$, $\epsilon_\perp = 2.3$, $\mathbf{E_0} = 3 \cdot 10^6$V/m $\mathbf{e_x}$, $w_0 = 0.5\mu$m, $\lambda = 1064$nm, $a = 0.5\mu$m, and $\epsilon_C = 1.7$.

V. CONCLUSIONS

In conclusion, we have presented and analyzed the mechanisms of laser trapping of small colloidal particles dispersed in a nematic liquid crystals, when their refractive index is low compared to the refractive indices of a liquid crystal. Depending on the laser power, the colloid is either trapped via its "birefringent cloud" at low power levels, or is attracted by a "ghost" colloid, created by laser-induced distortion of a director field. Above the threshold field for laser-induced Freedericksz transition we have observed two different types of trapping trajectories. The first type of trajectories is highly anisotropic, spider-like, and has been observed in approximately 80 percents of trapping experiments. The symmetry of the trajectories is consistent with a simple picture, where a colloid with its dipolar director field is attracted into the localized, highly distorted nematic field in the laser trap. Depending on the direction of the polarization of the light field, there is an "easy" direction, where the colloid is attracted by an apparent, Coulomb-like pair potential. A numerical analysis, where the elastic anisotropic attraction between the laser-distorted nematic and the deformed region, the anisotropic dielectric attraction of the laser polarization with distorted and optically anisotropic nematic, and the symmetric and repulsive interaction due to low index of the colloid are considered, shows a very

good agreement with experiments. It clearly shows, that the apparent, Coulomb-like interaction, is a result of the combination of these three interaction terms. We should also stress that screening of the laser trap-colloid interaction due to the presence of the confining walls should also be considered above certain range of separation. Finally, the symmetry properties of approximately 20 percent of trapping trajectories indicate quadrupolar director field around the colloids. This type of ordering has already been observed in other experiments [**?**], and the numerical analysis of trapping of quadrupolar-like colloids is left for possible future studies. Nevertheless, it should be stressed that already a selected choice of the experiments and their analysis show, that there are subtle force mechanisms, that have to be carefully considered in laser tweezers experiments in soft matter.

The authors would like to acknowledge the financial contribution of the European Commission under the project ALCANDO, contract G5MA-CT-2002-04023.

[] P. Poulin, H. Stark, T.C. Lubensky, and D.A. Weitz, Science **275**, 1770 (1997).
[] P. Poulin and D. Weitz, Phys. Rev. E **57**, 626 (1998).
[] Y. Ch. Loudet, P. Barois, and P. Poulin, Nature **407**, 611 (2000).
[] V. G. Nazarenko, A. B. Nych, and B. I. Lev, Phys. Rev. Lett. **87**, 075504, (2001).
[] I. I. Smalyukh, S. Chernyshuk, B. I. Lev, A. B. Nych, U. Ognysta, V.G. Nazarenko, and O. D. Lavrentovich, Phys. Rev. Lett. **93**, 117801, (2004).
[] M. Yada, J. Yamamoto, H. Yokoyama, Langmuir **18**, 7436(2002).
[] S. P. Meeker, W. C. K. Poon, Y. Crain, and E. M. Terentjev, Phys. Rev. E **61**, R6083 (2000).
[] S.L.Lopatnikov and V.A.Namiot, Zh. Eksp. Teor. Fiz. **75**, 361 (1978) [Sov. Phys. JETP **48**, 180 (1978)]
[] S. Ramaswamy, R. Nityananda, V. A. Raghunathan, J. Prost, Mol. Cryst. Liq. Cryst. **288**,175 (1996).
[] O. Kuksenok, R. W. Ruhwandl, S. Shiyanovskii, and E.M. Terentjev, Phys. Rev. E **54**, 5198 (1996).
[] T. C. Lubensky, D. Pettey, N. Currier, and H. Stark, Phys. Rev. E **57**, 610 (1998).
[] B. I. Lev and P. M. Tomchuk, Phys. Rev. E **59**, 591 (1999).
[] S. B. Chernyshuk, B. I. Lev, and H. Yokoyama, Zh. Eksp. Teor. Fiz. **120**, 871 (2001) [Sov. Phys. JETP **93**, 760 (2001)].
[] B. I. Lev, S. B. Chernyshuk, P. M. Tomchuk, and H. Yokoyama, Phys. Rev. E **65**, 021709 (2002).
[] H. Stark, Eur. Phys. J. B **10**, 311 (1999).
[] H. Stark, Physics Report **351**, 387 (2001).
[] D. Andrienko, G. Germano, and M. Allen, Phys. Rev. E **63**, 041701 (2001).
[] D. Andrienko, M. Allen, G. Skačej, and S. Žumer, Phys. Rev. E **65**, 041702 (2002).
[] O. Guzman, E. B. Kim, S. Grollau, N. L. Abbott, J. J. de Pablo, Phys. Rev. Lett. **91**, 235507(2003).
[] Jun-ichi Fukuda, M. Yoneya, H. Yokoyama, H. Stark, Colloids and Surfaces B: Biointerfaces **38**, 143(2004)
[] Jun-ichi Fukuda, H. Stark, M. Yoneya, H. Yokoyama,Phys. Rev. E **69**, 041706(2004).
[] P. Poulin, V. Cabuil, and D. Weitz, Phys. Rev. Lett. **79**, 4862 (1997).
[] M. Yada, J. Yamamoto, H. Yokoyama, Phys. Rev. Lett. **92**, 185501(2004)
[] I. I. Smalyukh, A. N. Kuzmin, A. V. Kachynski, P. N. Prasad, O. D. Lavrentovich, Appl. Phys. Lett. **86**, 021913(2005).
[] T. A. Wood, H. F. Gleeson, M. R. Dickinson, A. J. Wright, Appl. Phys. Lett. **84**, 4292(2004).
[] I. Muševič, M.Škarabot, D. Babič, N. Osterman, I. Poberaj, V. Nazarenko, and A. Nych, Phys. Rev. Lett. **93**, 187801(2004).
[] J. C. Loudet, P. Hanusse, P. Poulin, Science **306**, 1525(2004).
[] P.G. de Gennes and J. Prost, *The Physics of Liquid Crystals*, 2nd ed. (Oxford Science Publications, Oxford, 1993).
[] T. Tlusty, A. Meller and R. Bar-Ziv, Phys. Rev. Lett. **81** , 1738 (1998).
[] G. Chen, H. Takezoe and A. Fukuda, Liq. Cryst. 5, 341 (1989)
[] H.C. Van de Hulst, *Light Scattering by Small Particles*, (John Wiley & Sons, New York, 1957).
[] H. Stark, *Physics of Inhomogeneous Nematic Liquid Crystals: Colloidal Dispersions and Multiple Scattering of Light*, (Habilitationsschrift, 1999).
[] Yuedong Gu, N. L. Abbott, Phys. Rev. Lett. **84**, 4719(2000).